LOWLAND TECHNOLOGY INTERNATIONAL Vol. 3, No. 2, 43-57, December 2001
International Association of Lowland Technology (IALT), ISSN 1344-9656

APPLICATION OF GLOBAL OPTIMIZATION TECHNIQUE FOR CALIBRATING THE XINANJIANG WATERSHED MODEL

H. A. P. Hapuarachchi[1], Zhi-Jia Li[2], M. Ranjit[3] and Q. J. Wang[4]

ABSTRACT: The manual calibration process of the Xinanjiang model is extremely difficult and it can be a rather frustrating and time consuming exercise for an inexperienced person. Therefore, in recent years, researchers are exploring ways to incorporate 'expert knowledge' of conceptual watershed models into the automatic calibration procedures. Although there are many optimization techniques that can be applied for calibrating the Xinanjiang model, they are still not good enough to find a conceptually realistic and global optimum parameter set for the model. This paper presents a brief introduction to the Xinanjiang model and a research work on application of SCE-UA (Shuffle Complex Evaluation) global optimization technique for calibrating Xinanjiang watershed model using hydrological data of three catchments of different sizes and climatic conditions. Results show that the overall performance of SCE-UA method for calibrating the Xinanjiang model is very good. On the basis of the results derived from the calibration and verification stages, it demonstrates that SCE-UA is capable of finding a global optimum and conceptually realistic parameter set for the Xinanjiang model.

INTRODUCTION

The Xinanjiang hydrological model is a conceptual watershed proposed by Zhao et al. (1980). It has been applied to large basins in the humid and semi humid regions of China for daily rainfall runoff and rainstorm flood forecasting. Use of the model has also spread to other fields of application such as water resources estimation, design flood and field drainage, water project programming, hydrological station planning, water quality accounting etc.

The model consists with sixteen parameters. Usually the model is calibrated manually. The manual calibration requires detailed understanding of the model, which can only be obtained through many years of calibration experience. With training and good deal of experience, it is possible to obtain very good model calibrations using the manual approach. But, for the inexperienced and untrained persons, manual calibration can be a rather frustrating and time consuming exercise. This is mainly because the logic by which the parameters should be adjusted to improve the match is difficult to determine. The main weakness of manual calibration is that the absence of generally accepted objective measures of comparison which makes it difficult to know when the process should be terminated. Therefore, it is very essential to explore ways to incorporate 'expert knowledge' of calibrating Xinanjiang model into the automatic calibration procedures.

In this research, SCE-UA (Shuffle Complex Evolution) method, developed at the University of Arizona in 1992 (Duan et al. 1993), has been applied to calibrate the Xinanjiang

1 Doctoral degree candidate, College of Water Resources & Environment, Hohai University, Nanjing, CHINA.
2 Professor, ditto.
3 Researcher, Research Center for Applied Science and Technology, Tribhuvan University, Kathmandu, NEPAL.
4 Professor, College of Water Resources & Environment, Hohai University, Nanjing, CHINA.
Note: Discussion on this paper is opened until June 1, 2002.

model. This method is based on a synthesis of the best features from several existing methods, including the Genetic Algorithm and Simplex downhill search scheme (Nelder and Mead 1965). It introduces a new concept of complex shuffling. According to the literature, SCE-UA method is not problem specific and it is easy to handle. The method was designed specially for the purpose of dealing with the peculiar problems encountered in conceptual watershed model calibration (Duan et al. 1993, 1994). But it can generally be used for nonlinear optimization problems effectively as well. SCE-UA method is capable of handling high parameter dimensionality and it does not rely on the derivatives. The method has been used in various fields for optimization and reported exact results. Duan et al. (1994) indicate that SCE-UA method is not only effective but also efficient, compared with other existing global optimization methods, including the ARS (Adaptive Random Search) method and the Multi Start Simplex method (MSX).

In this paper, the structure of the SCE-UA algorithm is not discussed in detail. A detailed description of the method can be found in the literature (Duan et al. 1992, 1993).

STRUCTURE OF THE XINANJIANG MODEL

The main feature of the model is the concept of runoff formation on repletion of storage, which means that runoff is not produced until the soil moisture content of the aeration zone reaches the field capacity, and thereafter runoff equals the rain fall excess without further loss.

According to the model structure, runoff was separated to three components as surface runoff, inter flow and ground water flow. Based on the concept of runoff formation on the repletion of storage, the simulation of outflow from each sub-basin has four major parts.

1) Evapotranspiration, which generates the deficit of soil storage, which is divided into three layers: upper, lower and deeper.

2) Runoff production, which produces the runoff according to the rainfall and soil storage deficit.

3) Total runoff separation, which divides the above so determined runoff into three components: surface runoff, subsurface flow and groundwater flow.

4) Flow routing, which transfers the local runoff to the outlet of each sub-basin forming the outflow of the sub-basin.

Normally, the soil moisture deficit often varies from place to place. To provide a non-uniform distribution of tension water capacity throughout the basin, a tension water capacity curve has been introduced in Xinanjiang model.

The schematic diagram of the Xinanjiang model is shown in Fig. 1. All symbols inside the blocks are variables including inputs, outputs, state variables and internal variables and those outside of the blocks are parameters. 16 parameters in the Xinanjiang model are classified in the following way.

Evapotranspiration parameters: K, the ratio of potential evapotranspiration to the pan evaporation; WUM, the tension water capacity of upper layer; WLM, the tension water capacity of lower layer; C, the evapotranspiration coefficient of deeper layer.

Runoff production parameters: WM, the areal mean tension water capacity; B, the exponential of the distribution of tension water capacity; IM, the ratio of impervious area to the total area of the basin.

Runoff separation parameters: SM, the free water storage capacity; EX, the exponential of distribution water capacity; KG, the out flow coefficient of free water storage to the ground water flow; KI, the out flow coefficient of free water storage to the inter flow.

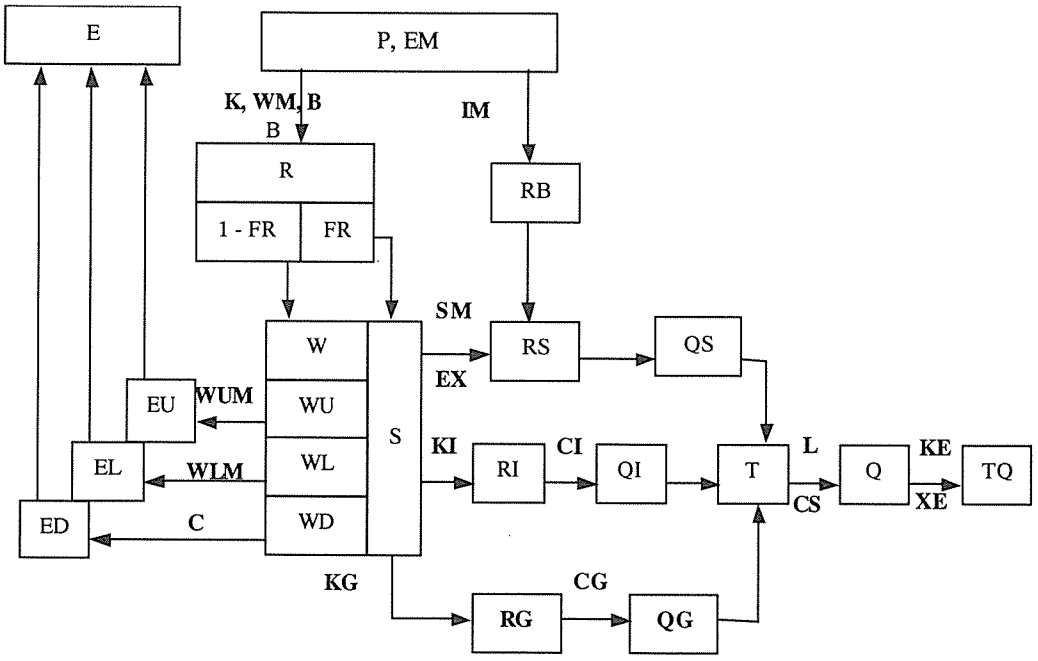

Fig. 1 Schematic diagram of Xinanjiang Model

Runoff concentration parameters: *CG*, the recession constant of ground water storage; *CI*, the recession constant of lower interflow storage; *CS*, the recession constant of channel network storage.

Muskingum parameters: *XE*, Muskingum weighting coefficient; *KE*, the residence time of water.

The inputs to the model are areal mean rainfall (*P*) and measured pan evaporation (*EM*). The outputs are the discharge from the whole basin (*TQ*), the actual evapotranspiration (*E*) which includes the three components from upper (*EU*), lower (*EL*), and deeper (*ED*) layers. The state variables are the areal mean free water storage (*S*) and the areal mean tension water storage (*W*), which has three components *WU, WL*, and *WD* in the upper, lower and deeper layers respectively. *RB* is the direct runoff from impervious area and *FR* is the runoff contributing area factor, which is related to *W*. The runoff produced from pervious area (*R*) is divided into three components, surface runoff (*RS*), interflow (*RI*) and groundwater flow (*RG*) respectively. The three components are further transferred into *QS, QI* and *QG* and together form the total inflow to the channel network of the sub-basin.

THEORETICAL BACKGROUND OF XINANJIANG MODEL

Evapotranspiration

The actual evapotranspiration of the basin is related to both the potential evapotranspiration and the soil moisture condition. The observed pan evaporation is input to the model and is converted to the actual evapotranspiration by multiplying *K*, the ratio of potential evapotranspiration to pan evaporation. Tension water storage in the basin at any moment corresponding to three layers, are *WU, WL* and *WD*. In this study it is assumed, until the uppermost layer tension water storage (*WU*) is exhausted, evaporation occurs at the potential rate equal to *K* times the pan evaporation rate.

$$EU = K \times EM \tag{1}$$

After exhausting the upper layer storage, any remaining potential evapotranspiration is applied to the lower layer. Actually, the efficiency should be lower than that of the rate of evapotranspiration from the upper layer. Therefore the efficiency is modified by multiplying with the ratio of actual storage WL to the capacity storage WLM of that layer.

$$EL=(K \times EM - EU) \times WL/WLM \tag{2}$$

When the lower layer tension water storage is reduced to a value, $WL=C \times WLM$, the deeper layer evapotranspiration begins with further reduced rate,

$$ED=C \times (K \times EM - EU) - EL \tag{3}$$

where *EU, EL* and *ED* are the evapotranspiration from the upper, lower and deeper layers respectively.

Runoff Production

The concept that the runoff production occurs at a point in the sub basin only on the repletion of the tension water storage at that point is applied in the Xinanjiang model. Considering the entire watershed, things are more complicated and the moisture deficit often varies from place to place. To represent this non-uniform distribution of tension water capacity throughout the basin or sub basin, a tension water capacity curve is introduced to the model (Fig. 2).

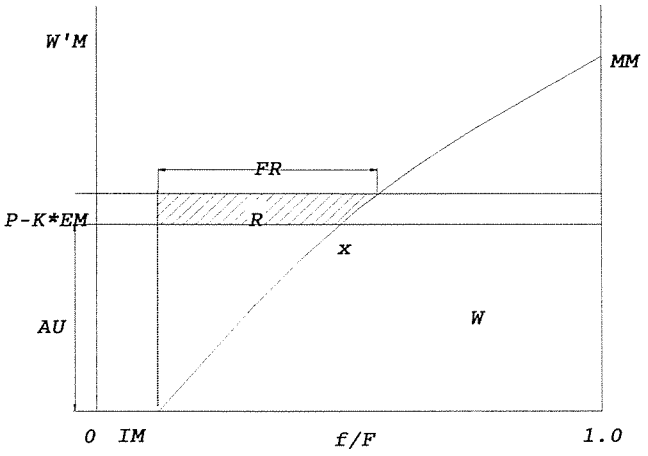

Fig. 2 The distribution of the tension water capacity in the basin

Tension water capacity curve is a curve of moisture capacity in the aeration zone at various points in the watershed arranged in ascending order of magnitude, plotted against the corresponding area (see Fig. 2). Here *f* denotes the area of which the storage capacity at any point less than or equal to *W'M* and *F* denotes the total area of the watershed.

The tension water capacity curve is a monotone increasing function, and should be limited on both ends in the range of $0 \leq W'M \leq MM$ for humid regions, where *MM* is the maximum storage capacity at any point in the watershed. The area under the curve represents the areal mean tension water capacity in the aeration zone of the entire watershed, which is denoted by *WM*.

$$WM = \int_{IM}^{1} W'M \, d\left(\frac{f}{F}\right) \tag{4}$$

The value f/F represents the proportion of the pervious area of the sub basin whose tension water capacity is less than or equal to the value of the ordinate $W'M$.

In Fig. 2, point x on the curved line represents the state of the sub basin at any time. The area on the right and below the point x is proportional to the areal mean tension water storage W. That means, each point in the sub basin is either at capacity tension (points to the left of x) or at a constant tension state (points to the right of x). The tension water capacity at a point, $W'M$ varies from zero to a maximum of MM according to the following relationship.

$$\left(1-\frac{f}{F}\right) = \left(1-\frac{W'M}{MM}\right)^{B} \times (1-IM) \tag{5}$$

There are two parameters remaining to be determined in this equation, namely, B and MM. From Eq. (5), the mathematical expression of the rainfall-runoff relation can be derived as follows:

$$WM = \int_{0}^{MM} \left(1-IM-\frac{f}{F}\right) d(W'M) \tag{6}$$

The areal mean tension water capacity, WM constitutes an alternative parameter to the maximum of MM, and related through the parameter B. By integrating equation (6), the following expression can be obtained.

$$MM = WM \times \frac{(1+B)}{(1-IM)} \tag{7}$$

The ordinate "AU" corresponding to W on the tension water capacity curve can be determined by,

$$W = \int_{0}^{AU} \left(1-IM-\frac{f}{F}\right) d(W'M) \tag{8}$$

Integrating (8) we obtain,

$$AU = MM\left[1-\left(1-\frac{W}{WM}\right)^{\frac{1}{1+B}}\right] \tag{9}$$

When rainfall exceeds evaporation, the ordinate AU in Fig. 2 increases and meantime x moves upwards along the curve. As a result, runoff is generated proportional to the area shaded to the left and above the point x. Runoff production can be represented mathematically as follows.

Let $A=AU+(P-K*EM)$, then runoff amount R is equal to

$$R = \int_{AU}^{A} \left(\frac{f}{F} - IM \right) d(W'M) \tag{10}$$

Through integration, two cases of runoff equation are given.
If $A < MM$ then,

$$R = P - K \times EM - WM + W + WM \times \left(1 - \frac{(P - K \times EM + AU)}{MM}\right)^{(1+B)} \tag{11}$$

Otherwise,

$$R = P - K \times EM - WM + W \tag{12}$$

It is clear that as long as the tension water capacity curve is given, and B and WM are known, the rainfall-runoff relation can be completely determined.

Runoff Separation

In Fig. 2, the runoff R produced in a wet period should be furtherly separated into its three components, RS, surface runoff, RI, interflow contribution and RG, the ground water contribution.

$S'M$ is assumed to be distributed between zero and maximum values of MS in a parabolic manner over FR, the portion of the sub basin which is currently producing runoff. The distribution curve is illustrated in Fig. 3.

$$\left(1 - \frac{f}{FR}\right) = \left(1 - \frac{S'M}{MS}\right)^{EX} \tag{13}$$

It is also assumed that the current state of the sub basin can be represented by the point x on the parabola implying that the points of left to x are at free water capacity storage and that of right to x are at constant free water storage state. The points to the right of x are below capacity level. It is convenient to use areal mean free water storage capacity SM, instead of MS as a parameter.

$$MS = SM\,(1 + EX) \tag{14}$$

By integrating the equation (13) and substituting SM from equation (14), the equivalent free water storage S over the runoff producing area FR can be obtained as follows.

$$\left(1 - \frac{S}{SM}\right) = \left(1 - \frac{BU}{MS}\right)^{(1+EX)} \tag{15}$$

The total runoff produced R, expressed as a depth $P–K\times EM$ over the runoff producing area of the sub basin is applied by adding $P–K\times EM$ to BU in Fig. 3, yielding a contribution RS to surface runoff.

If $(BU + P - K \times EM) < MS$ then

$$RS = \left\{ P - K \times EM - SM + S + SM \times \left(1 - \frac{(P - K \times EM + BU)}{MS} \right)^{(1+EX)} \right\} \times FR \tag{16}$$

Otherwise,

$$RS = (P - K \times EM + S - SM) \times FR \tag{17}$$

The reminder of R becomes an addition ΔS, to the free water storage S and later contributes RI laterally to interflow and RG vertically to ground water according to the following relations.

$$RI = S \times KI \times FR \tag{18}$$

$$RG = S \times KG \times FR \tag{19}$$

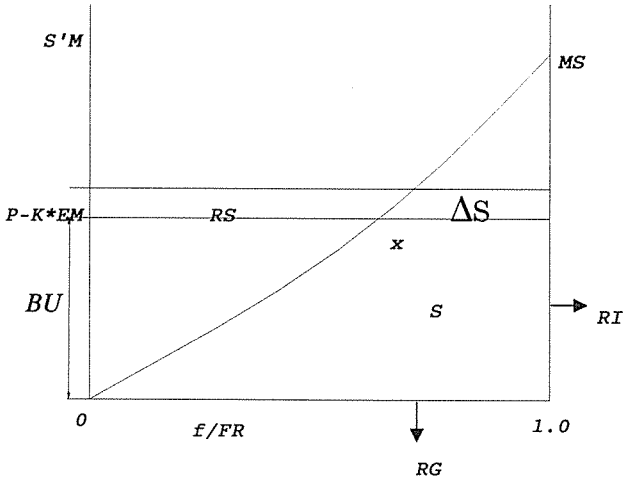

Fig. 3 Separation of runoff components

Flow Concentration in Sub Basins

The surface flow is several times faster than the interflow and ground water flow. Therefore, surface runoff RS passes to the channel system as TS without any modifications. RI and RG are routed through linear reservoir representing interflow and ground water storage respectively. The outflows TI and TG from these reservoirs are determined by the following equations.

$$TI_{(t)} = TI_{(t-1)} \times CI + RI_{(t)} \times (1 - CI) \tag{20}$$

$$TG_{(t)} = TG_{(t-1)} \times CG + RG_{(t)} \times (1 - CG) \tag{21}$$

Where t is current time and (t-1) is previous time interval.
The total sub basin inflow T can be represented as follows:

$$T = TS + TI + TG \tag{22}$$

The channel network routing within a sub basin is represented by the convolution of T with an empirical unit hydrograph or by "Lag and Route" model with parameters L and CS. Here L is the lag time and CS is the storage coefficient of the linear reservoir. The out flow Q from the sub basin can be obtained.

Flow routing from the sub basin outlets to the whole basin outlet is achieved by applying Muskingum method to successive reaches.

A detailed description of the model is available in the literature (Zhao et al. 1980).

APPLICATION OF SCE-UA METHOD

The SCE-UA algorithm contains many parameters that control the probabilistic and deterministic components of the method. These parameters should be carefully selected for the optimal performance of the algorithm. Actually, the optimum values of these parameters depend on the type of the problem. Practical observation showed that the following values can be generally used as default. $m=(2a+1)$; $q=(a+1)$; $d=1$, $z=(2a+1)$. Where m is the number of points in a complex, q is the number of points in a sub complex, p is the number of complexes, d is the number of consecutive offspring generated by each sub complex, z is the number of evolution steps taken by each complex and a is the number of parameters to be optimized on. Hence, the only variable to be specified by the user is the number of complexes p. Theoretically m can be any value greater than one. If m is chosen too large, it may effect in excessive use of the computer processing time with no longer effectiveness. q can be in the range 2 q m. The required number of complexes, p depends on the type of the problem (Duan et. al. 1993, 1994). Large number of complexes is needed for highly nonlinear problems.

For the calibration of the Xinanjiang model, the following parameters were kept constant for all catchments as: $a=13$, $p=3$, $m=27$, $q=14$, $d=1$ and $z=27$.

OBJECTIVE FUNCTIONS

Three objective functions have been used for the calibration. Previous research works show that the results obtained using absolute error as objective function are more stable than that of least squares. Therefore, in this study only the absolute error for objective functions is considered.

First function calculates the relative absolute accumulated volume error over the whole period. This helps to keep the water balance throughout the period. Here Q_{obs} is the observed discharge, Q_{cal} is the calculated discharge and n is number of observations.

$$Obj1 = \left| \frac{\sum_{i=1}^{n} Q_{obs}(i) - \sum_{i=1}^{n} Q_{cal}(i)}{\sum_{i=1}^{n} Q_{obs}(i)} \right| \tag{23}$$

Second objective function indicates the mean relative absolute error, being the sum of the absolute error of prediction normalized by dividing by the measured discharge.

$$Obj\,2 = \frac{1}{n} \sum_{i=1}^{n} \left| \frac{Q_{obs}(i) - Q_{cal}(i)}{Q_{obs}(i)} \right| \tag{24}$$

Third objective function calculates the absolute mean logarithmic error. This can treat the lagging of the hydrograph. One is introduced in the equation for eliminating the *log* value becoming undefined.

$$Obj\,3 = \frac{1}{n}\sum_{i=1}^{n} \log\left(\left|\frac{Q_{obs}(i) - Q_{cal}(i)}{Q_{obs}(i)}\right| + 1\right) \tag{25}$$

The main objective function (F) is defined as the combination of above mentioned three objective functions. It is assumed that the combination would give a better result than individual use.

$$F = \sum_{i=1}^{y} \left(Obj1\,(i) + Obj2\,(i) + Obj3\,(i)\right) \tag{26}$$

where y is the number of years.

STATISTICAL INDICES

Two statistical indices selected to compare the performance of the model calibrated with SCE-UA method are D_y and *%Err*.

$$D_y = 1 - \left(\frac{\sum_{i=1}^{n}(Q_{obs}(i) - Q_{cal}(i))^2}{\sum_{i=1}^{n}\left(Q_{obs}(i) - \bar{Q}_{obs}(i)\right)^2}\right) \tag{27}$$

where Q_{obs} is daily mean observed discharge. *%Err* is a value for checking the water balance throughout the year. The error is obtained as a percentage and depending on the sign (positive or negative), the calculated discharge can be lower or higher than the observed discharge.

$$\%Err = \left(\frac{\sum_{i=1}^{n} Q_{obs}(i) - \sum_{i=1}^{n} Q_{cal}(i)}{\sum_{i=1}^{n} Q_{obs}(i)}\right) \times 100 \tag{28}$$

Theoretically, *%Err* can be positive or negative, depending on whether observed discharge is greater than or less than the calculated discharge.

STOPPING CRITERIA OF ITERATIONS

Three criteria have been used for the termination of the iterative process. The calibration process is terminated if one or more of the following criteria are satisfied.

1) The search is stopped when the algorithm is unable to appreciably improve 0.01 percent of the value of the objective function over five iterations. It could mean that a very flat region of the response surface has been reached.

2) The search is stopped when the algorithm is unable to appreciably change the parameter values and simultaneously improve the function value over five iterations. While this can indicate arrival at an optimum, it could also mean only that a region of high parameter interaction (long narrow valley) on the response surface has been reached.

3) Since the computer time is limited and, to ensure that the algorithm does not somehow enter a finite loop, the search is terminated if the maximum number of iterations (20,000) is exceeded, unless the parameter or function convergence criteria are met first.

TEST CATCHMENT'S CHARACTERISTICS

Three catchments of different size and climatic conditions were chosen (see Table 1). Two of them known as Bagmathi and Tamor are located in Nepal and Misai is located in China. Bagmathi and Tamor basins were calibrated with four years of hydrological data and for Misai, five years hydrological data have been used. Two years of hydrological data were used in the validation stage for all catchments.

The Bagmathi River is the principal river of the Bagmathi watershed and lies between the Koshi and Gandaki watersheds in central Nepal. Nearly 45% of the watershed area lies in the Mountain physiographic zone. Approximately 30% of the watershed lie in the Siwalik zone and the remaining 25% represents the Terai zone. Soils on the mountain slopes of Upper and Middle Bagmathi basins are relatively stable and thick (0.5 to 1.5 m). Soils are better developed in the valley floor of Kathmandu in the Upper Bagmathi Basin. Nearly 42% of the watershed area in under agriculture, 46% under forest cover and 14% occupied by degraded shrub land and grazing land. Nearly over 60% of the river discharge takes place in the wet monsoon season and the dry season contribution is less than 40%. It is estimated that more than 90% of the monsoon rain is diverted to the streams.

Table 1 General information about the three catchments

Catchment	Area (km^2)	Test mode	Total No. of days	Mean Rainfall (mm/day)	Mean pan Evaporation (mm/day)	Mean Discharge (mm/day)	Country	Catchment condition
Misai	797.0	C	1826	4.87	2.06	3.14	China	Semi wet
		V	731	4.91	2.14	3.37		
Tamor	5797.7	C	1461	8.64	4.38	5.27	Nepal	Semi wet
		V	730	8.64	4.38	5.50		
Bagmathi	2817.6	C	1461	4.71	3.09	3.67	Nepal	Semi wet
		V	730	5.30	3.09	4.23		

C- Calibration & V- Verification

Tamor River is located in the Lesser (middle hills) and Higher Himalayas (high mountains) of eastern Nepal. The river has the highest flow of 920 m^3/sec in July and the lowest flow of 52 m^3/sec in March. The annual precipitation is about 1,100 mm in the southern part of the valley and 1,000 mm in the upstream areas. Above 3,000 m elevation, precipitation is characterized by drizzling and snows fall. Above 80% of the annual rainfall occurs between June and September. Land use distribution shows that 35% of the total area is covered by forest, 25% by cultivated land, 15% by water bodies and 25% by rocks. The mountain areas in the north exceed an altitude of 3,000 m. The hilly areas consist of ridges and steep slopes including the Mahabharat range and Siwalik hills.

Misai watershed (in Zhejiang province, China) is located south of the 29^0 30' latitude and west of the 118^0 30' longitude. The area is mountainous and with thick vegetation cover. The upper layer soil is highly permeable. Therefore the infiltration capacity is higher. Normally, the ground water flow is high and it covers about 40% of yearly runoff.

The area is semi humid and the precipitation is fairly high. Yearly average rainfall is about 1,500 ~ 2,000 mm. Yearly runoff coefficient is about 0.7~0.8. Monsoon period is from April to June during which the amount of precipitation is about 60% of yearly precipitation. Mid summer begins from July during which it is a little dry and sometimes heavy rainfalls with high intensity might occur for a short period. Rainfall distribution is uneven over the catchment. There is very less rain during November to February.

RESULTS

Three independent trials were conducted for each catchment with different initial conditions and different initial seeds. Parameters *K, IM, B, WUM, WLM, C, SM, EX, CG, CI, CS, KG, XE* were calibrated by using the SCE-UA method while *WM* and *KE* were kept constant. Since we use the daily model, *KE*=24 hrs for all iterations. *WM* value was chosen in such a way that *WUL+WUM+WUD* value would not become negative. *KI* value was chosen according to the relationship, *KI+KG=0.7*. All the iterations were stopped given the function convergence stopping criteria was satisfied.

DISCUSSION OF RESULTS

Two statistical indices (D_Y and *%Err*) as mentioned above, have been used to compare the performance of the SCE-UA method. A careful inspection of tables 2, 3, 4 and 5 reveals that statistics and parameter values give nearly similar results in all three trials in each catchment. Even though the parameter values are not the same, the error bound is negligible. In fact the accuracy can be enhanced by changing the tolerance of stopping criteria. Figures 4, 5, and 6 shows the fit of the calculated and observed river discharges for Misai, Tamor and Bagmathi catchments respectively. Only selected period (one year) of the hydrograph is shown for the convenience. It is clear that modeled discharge fits well with the observed discharge in the three catchments.

The best statistics are shown in the Bagmathi (Table 5) basin. Both the calibration and validation results are acceptable. Only in 1990 statistics are not good. It may happen due to the data errors. But it is worth to note that achieving better statistics at the calibration stage does not guarantee getting parameter sets always with a stronger physical basis.

Considering the Misai basin (Table 2), the parameter values obtained in three trials are almost similar. It is clear from Fig. 4 that calibration results of Misai watershed are very good. But validation results are not very good compared with that of Bagmathi basin. Topographic conditions and accuracy of discharge data might cause this difference. Considering the topography, Bagmathi basin is located in mountainous area, whereas Misai is comparatively in flat area.

In fact, compared to the other two basins, Tamor basin calibration results are not very good (Table 4). Tamor River is a snow-fed river and originates entirely within the territory of Nepal. The northern area (approximately north latitude 27^0 30') lies in the higher Himalayan Zone and has a very rugged topography, steep slopes and dominated by glacial-per glacial geomorphology. A number of glacier and high altitude lakes are located in this basin. Snow-fed area comprises about 20% of the total basin area. These factors may cause for the poor

calibration results since Xinanjiang model is incapable of accounting snow. However, the model should be applied with much caution in the areas with extreme geographical features like Tamor basin even though the failure to use the model can partly be attributed to the inaccuracy of the observed discharge data.

Based on the results, it is clear that Xinanjiang hydrological model can be well applied to the selected Bagmathi basin, and Tamor basin (Nepal) that represent various climatic and geographical zones of Nepal.

From these results it may conclude that the SCE-UA method is capable of finding a conceptually realistic and global optimum parameter set for the Xinanjiang watershed model. Also our results clearly show that SCE-UA can handle high parameter dimensions and achieve the global convergence in the presence of multiple regions.

It is noted that the initial conditions of the watershed (*W, WUM, WUL, S, FR, QS, QI, QG*) should be carefully selected such that the calculated discharge at the beginning of the year is nearly equal to the observed discharge. Invalid initial data may cause negative mean tension water storage (*W*) in the iterative process. As a result, the search may trap in local optimums or the computational time can be longer.

Table 2 Calibrated values for Xinanjiang model parameters using SCE-UA method

	Misai			Tamor			Bagmathi		
Trial No.	**#1**	**#2**	**#3**	**#1**	**#2**	**#3**	**#1**	**#2**	**#3**
K	0.922	0.922	0.922	1.275	1.268	1.274	0.554	0.553	0.544
IM	0.001	0.001	0.001	0.123	0.124	0.123	0.129	0.114	0.151
B	0.080	0.080	0.080	0.700	0.700	0.700	0.091	0.105	0.07
WUM	34.999	34.996	34.986	16.368	17.529	15.648	10.735	10.500	11.402
WLM	64.997	65.012	65.026	64.993	64.986	64.982	31.905	28.050	28.231
C	0.350	0.350	0.350	0.019	0.018	0.020	0.136	0.138	0.128
SM	9.372	9.595	9.330	27.999	27.997	27.997	24.088	21.529	25.571
EX	0.800	0.815	0.801	0.775	0.758	0.767	0.710	0.689	1.671
CG	0.999	0.999	0.999	0.989	0.990	0.989	0.998	0.998	0.998
CI	0.890	0.890	0.891	0.941	0.942	0.941	0.947	0.948	0.949
CS	0.281	0.276	0.286	0.242	0.242	0.240	0.064	0.065	0.195
KG	0.119	0.117	0.117	0.302	0.299	0.302	0.055	0.058	0.063
XE	0.485	0.488	0.488	0.120	0.122	0.118	0.318	0.330	0.301
KI	0.581	0.583	0.583	0.398	0.401	0.398	0.645	0.642	0.637
WM	125	125	125	125	125	125	125	125	125
KE	24	24	24	24	24	24	24	24	24

Table 3 Calibration and validation results of Misai watershed

Mode	Year	Precipi. (mm)	Evapo. (mm)	*RS* (mm)	*RI* (mm)	*RG* (mm)	Q_{obs} (mm)	Q_{cal} (mm)	Trial *% Err*	#1 D_Y	Trial *% Err*	#2 D_Y	Trial *% Err*	#3 D_Y
Calibration	1982	1649.23	622.16	535.44	371.11	74.81	1042.188	988.90	5.143	0.922	5.119	0.923	5.079	0.921
	1983	2513.94	609.74	1290.88	539.02	108.65	1893.342	1917.26	-1.252	0.891	-1.247	0.891	-1.291	0.890
	1984	1727.68	617.53	559.61	426.43	85.96	1076.249	1076.25	0.000	0.894	0.000	0.894	0.000	0.893
	1985	1581.79	661.33	481.48	363.97	73.37	934.855	931.64	0.339	0.851	0.343	0.849	0.348	0.851
	1986	1447.20	707.13	417.25	301.58	60.79	798.251	798.26	-0.001	0.909	0.000	0.911	-0.001	0.908
Validation	1987	2062.11	637.23	777.67	546.32	110.25	1354.58	1415.32	-4.471	0.875	-4.491	0.874	-4.539	0.875
	1988	1524.64	584.13	577.56	361.75	72.57	1106.52	1030.15	6.903	0.860	6.913	0.862	6.889	0.859

Table 4 Calibration and validation results of Tamor watershed

Mode	Year	Precipi. (mm)	Evapo. (mm)	*RS* (mm)	*RI* (mm)	*RG* (mm)	Q_{obs} (mm)	Q_{cal} (mm)	Trial *% Err*	#1 D_Y	Trial *% Err*	#2 D_Y	Trial *% Err*	#3 D_Y
Calibration	1989	2663.20	1232.07	536.54	514.95	384.62	1581.93	1395.32	11.726	0.934	11.819	0.934	11.774	0.935
	1990	3368.51	1335.68	1025.19	574.89	433.86	2101.59	2027.77	3.467	0.940	3.513	0.940	3.486	0.940
	1991	3544.56	1241.83	1106.21	682.67	515.20	2217.16	2301.94	-3.459	0.947	-3.721	0.947	-3.915	0.947
	1992	3052.42	1164.71	912.94	555.47	419.21	1795.55	1891.39	-4.883	0.915	-5.215	0.914	-5.457	0.914
Validation	1993	3109.85	1256.43	855.45	568.62	428.74	1902.61	1849.36	2.800	0.932	2.835	0.931	2.754	0.932
	1994	3196.44	1234.07	952.74	576.25	435.14	2117.02	1978.6	6.425	0.950	6.766	0.949	6.302	0.950

Table 5 Calibration and validation results of Bagmathi watershed

Mode	Year	Precipi. (mm)	Evapo. (mm)	*RS* (mm)	*RI* (mm)	*RG* (mm)	Q_{obs} (mm)	Q_{cal} (mm)	Trial *% Err*	#1 D_Y	Trial *% Err*	#2 D_Y	Trial *% Err*	#3 D_Y
Calibration	1989	1598.63	402.68	560.30	570.01	52.03	1371.93	1371.89	0.000	0.861	0.007	0.848	0.000	0.895
	1990	2167.58	498.98	758.23	826.49	75.43	1634.50	1747.12	-6.949	0.885	-6.883	0.881	-6.837	0.884
	1991	1380.18	423.20	396.18	515.74	47.07	1033.79	1033.79	0.000	0.855	0.000	0.855	0.000	0.859
	1992	1732.02	431.91	585.40	654.02	59.69	1328.66	1328.66	0.000	0.842	0.000	0.835	0.000	0.837
Validation	1993	1977.19	470.27	664.87	775.43	70.52	1556.92	1584.33	-1.992	0.919	-1.775	0.910	-1.728	0.926
	1994	1896.15	420.77	659.52	747.71	67.99	1528.93	1516.99	0.787	0.833	0.770	0.817	0.780	0.836

Note: The values of Precipitation, Evapotranspiration, *RS, RI, RG*, Observed Discharge, and Calculated Discharge in tables 3,4 &5 are average values obtained in three trials.

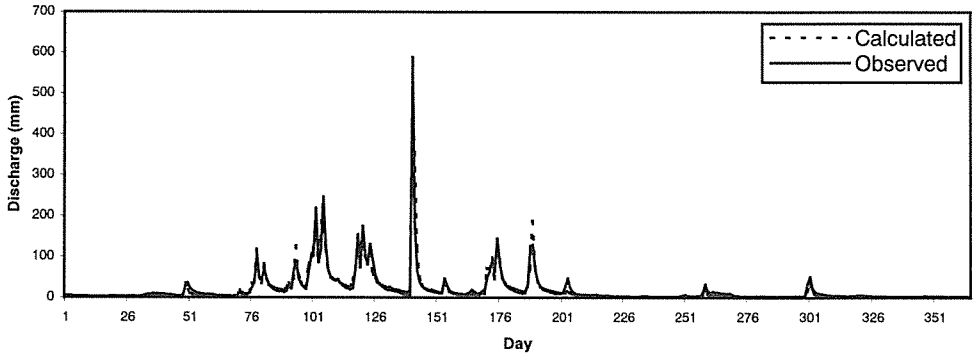

Fig. 4 Discharge hydrograph of Misai watershed for the data from Jan. to Dec. 1986

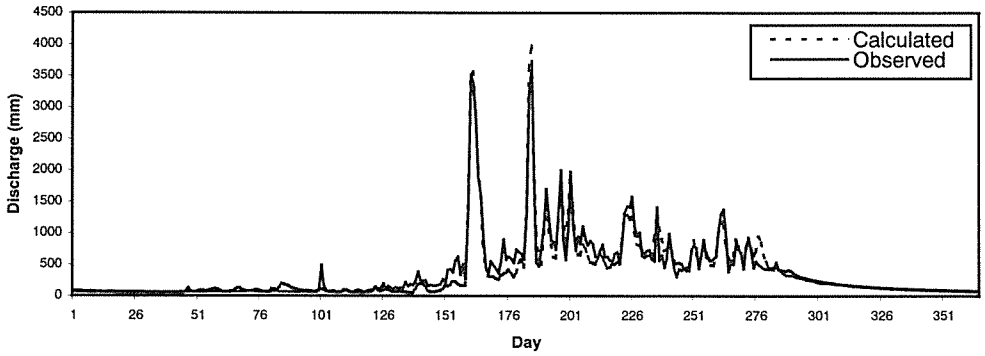

Fig. 5 Discharge hydrograph of Tamor watershed for the data from Jan. to Dec. 1990

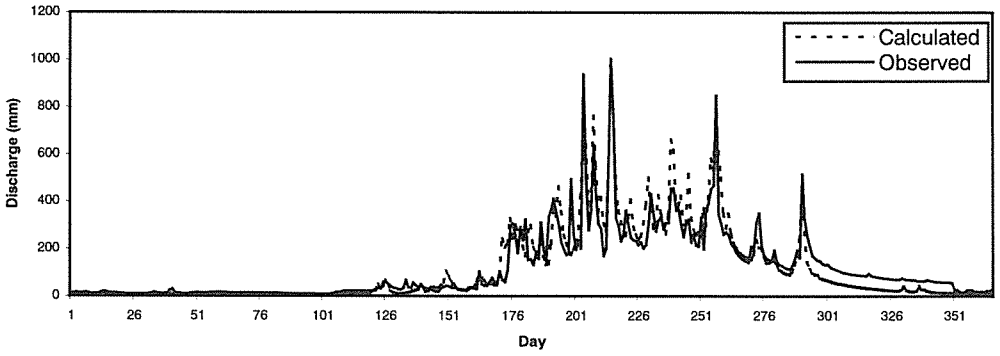

Fig. 6 Discharge hydrograph of Bagmathi watershed for the data from Jan. to Dec. 1992

CONCLUSIONS

A review of the essential concepts of the Xinanjiang model and the application results of SCE-UA method for calibrating the Xinanjiang model using hydrological data of three catchments of different climatic conditions, are presented in this paper. Based on the results obtained, the following conclusions can be drawn.

1) Overall performance of SCE-UA method for calibrating the Xinanjiang model is good. On the basis of the results derived from the calibration and verification stages, it seems that

SCE-UA is capable of finding a global optimum and conceptually realistic parameter set for the Xinanjiang model.

2) The Xinanjiang model can be successfully applied in semi wet catchments of Nepal. But the performance of the model result in snow fed areas is poor.

3) The objective function plays a major role in calibrating Xinanjiang watershed model. Therefore a combination of proper objective functions is recommended. Changes in objective function may direct the search process in certain direction.

4) The Xinanjiang model parameter boundary values should be carefully selected such that they represent the possible smallest range that could reach the global optimum. Especially the boundary values of parameters like *K, IM* etc. that have a physical meaning, should be selected by considering the real situation of the watershed. More attention should be paid for fixing the value of *WM* such that the value of *W* would not be negative in the iterative process.

5) SCE-UA method is capable of handling high parameter dimensionality and it does not rely on the derivatives. On the other hand, in the SCE-UA algorithm, only *p,* number of complexes, is the main variable. All other parameters can be fixed as default values. Therefore less knowledgeable user would be good at choosing SCE-UA for calibrating the Xinanjiang model.

REFERENCES

Duan, Q., Sorooshian, S. and Gupta, V. K. (1992). Effective and efficient global optimization for conceptual rainfall-runoff models. Water Resource Research. 28(4): 1015-1031.

Duan, Q., Sorooshian, S. and Gupta, V. K. (1994). Optimal use of SCE-UA global optimization method for calibrating watershed models. Journal of Hydrology. 158: 265-284.

Duan, Q. Y., Gupta, V. K. and Sorooshian, S. (1993). Shuffled complex evolution approach for effective and efficient global minimization. Journal of optimization theory and applications. 76(3): 501-521

Fryer, M. J. and Greenman, J. V. (1987). Optimization theory. Edward Arnold Pty Ltd.

Gan, T. Y. and Biftu, G. F. (1996). Automatic calibration of conceptual rainfall-runoff models: Optimization algorithms, catchment conditions and model structure. Water Resources Research. 32: 3513-3524.

Hapuarachchi, H. A. P. (2000). Application of Evolutionary Algorithms for Calibrating Xinanjiang Watershed Model. Master degree Thesis. Hohai University. Nanjing, China.

James, L. K. and Joe, H. M. (1973). Optimization Techniques with Fortran. McGraw-Hill Co.

Nelder, J. A., Mead, R. (1965). A simplex method for function minimization. Computer Journal. 7(4): 308-313.

Ranjit, M. (2001). Application of Xinanjiang Model in the Nepalese Terrain and Optimization of parameters. Master Degree Thesis. Hohai University. Nanjing, China.

Sancheti, D. C. and Kapoor, V. K. (1981). Statistics, Theory, methods and application. Sultan Chand & Sons.

Yapo, P. O., Gupta, H. V. and Sorooshian, S. (1998). Multi-Objective Global Optimization for Hydrologic Models. Journal of Hydro. 204: 83-97.

Zhao, R. J. (1992). The Xinanjiang Model applied in China, Journal of hydrology. 135: 371-381.

Zhao, R. J., Zhuang, Y. L., Fang, L. R., Liu, X. R. and Zhang, Q. S. (1980). The Xinanjiang Model. Hydrological forecasting proceedings of the Oxford Symposium. IAHS Publ. 129: 351-356.